

PARAMETRIC OPTIMISATION OF RESISTANCE WELDING THERMOPLASTICS-BASED COMPOSITES VIA COMPUTATIONAL AND EXPERIMENTAL APPROACHES

Jie Pu¹, Yunhao Liang^{1,2}, Yu Jia³ and Yu Shi²

¹ Department of Physical, Mathematical and Engineering Sciences, University of Chester, Parkgate Rd, Chester, CH1 4BJ, UK

² Leeds Institute of Textiles and Colour, School of Design, University of Leeds, Woodhouse Lane, Leeds, LS2 9JT, UK

³ School of Engineering and Applied Science, Aston University, Aston St, Birmingham, B4 7ET, UK

Keywords: Resistance welding, Finite Element Analysis, Heat transfer, Thermal uniformity.

ABSTRACT

In this study, the resistance welding process for carbon fibre reinforced thermoplastic composites (FRTPC) has been parametrically investigated through simulation and experiment processes. Heat transfer of resistance welding was studied computationally to generate optimum welding parameters. By applying a transient three-dimensional heat transfer model on COMSOL Multiphysics, evolution of temperature in the joint during welding process was simulated with various combinations of power densities and clamping distances. From different combinations of parameters, two main characteristics of heat transfer were revealed, which consequently resulted in various melting degree, uniformity of temperature upon welding interface, and heat penetrating through laminates in thickness direction. Based on optimum parameters, experimental welding tests were conducted, and mechanical tests showed that lap shear strength is proportional to melting degree but is independent of thermal penetration.

1 INTRODUCTION

Previous decades have witnessed an extraordinary growth in the application of FRTPC in aerospace, marine and automotive industries for their promising properties of easy storage, diverse manufacturing methods, high reparability and potential recyclability[1–3]. The most advantage of FRTPC over traditional thermoset composites is the reformability and recyclability through melting processes, which also enables composite parts to be joined by the welding process. The application of welding strategy in joining FRTPC parts can benefit the integration of designs in composites and reduce the chance of stress concentration after joining, compared with traditional adhesion method, resulting in a higher structural performance, reliability, and safety. The heating approaches applied in welding composite processes have been continuously developed, such as generating heat from electromagnetic, frictional, radiative, and ultrasonic energies. Among them, the resistance welding (RW), using the heat generated by a heating element upon the application of electric voltage, has been identified as one of the most popular welding technologies. This is because it features short cycle times and requires relatively inexpensive equipment [4,5].

The RW process is described as melting materials and then cooling under an adequate pressure [6] to consolidate and produce a reliable joint. Extensive researching work has been performed to investigate those key parameters affecting welding quality both computationally and experimentally. Within those parameters, heating element (HE) plays an important role in welding process as a heat generator and an intermedia to bond adherends in association with the adherent. Carbon fibre heating elements have been widely attempted due to the electrically conductive ability and good compatibility to maternal laminates[7,8]. However, this application is partially restricted by the nature of fibre induced poor weld reproducibility and problematic electrical connections [9]. Hou et al. [10] used stainless steel for joining polyetherimide(PEI) composite, which introduced good electric conductivity and a more homogeneous temperature distribution at the bonding interface. Recently, the space industry explored heating elements made of conductive polymer-based nanocomposite [11], to achieve welding with a capability of low-

density and anti-corrosion. However, mechanical performance of welded joints is expected to be improved.

From the perspective of welding process parameters, such as pressure, power, heating time and clamping distance have been regarded as the main factors affecting the welding quality [1,6,12]. The applied pressure is necessarily determining a high-quality welding that prevents de-consolidation during melting and a range of pressure from 0.4 to 1.2 MPa have been reported[6,13–15]. The power level (also known as power density) and heating time working together as a function of welding energy predominate the welding quality. Previous studies [13–15] revealed that lap shear strength of samples welded by a defined power density increased dramatically with the heating time increasing. Nevertheless, decrease in the lap shear strength is seen due to the overheating which induced degradation of materials. Based on that, heat transfer simulation is applied to predict thermal distribution [4,16–18] at a welding interface. By considering the impacts from heating element configurations, Talbot et al. [19] conducted a parametric study by a transient thermal model to identify how temperature distribution and melting degree are influenced by clamping distance.

In this study, we propose a heat transfer simulation to investigate thermal evolution volumetrically at welding interface and in laminates with multiple combinations of power densities and clamping distances. The heating element applied in this study is a stainless-steel mesh with the diameter of 0.03 mm and the aperture of 0.9 mm. Furthermore, the model simulates the generation and transfer of heat. Thereafter, the melting degree of the materials and the thermal gradient, at the welding interface and along the thickness direction of the joint sample, are analysed. The optimum welding parameters are then obtained and used for experimental operations. Mechanical performance of joints welded by designated parameters are evaluated, analysed, and discussed.

2 METHODOLOGY

The schematic graph of the welding system for a single lap shear specimen used in both the computational simulation and the experimental operation is depicted in Figure 1 (a), The investigated welding parameters are power density, clamping distance and pressure applied in the welding region. It is noteworthy that the welding pressure is fixed at a confident value of 0.4 MPa according to previous works[4,14,20] and therefore, will not be considered in simulation.

To predict melting condition in welded joints, a heat transfer model is established as shown in Figure 1 (b). Three main heat-transfer mechanisms are considered in the model, i.e., thermal conduction, convection, and radiation, to simulate how temperature develops on welding interface due to variation of welding parameters. In Figure 3 (b), free convection in the model is assumed to be affected in vertical and horizontal directions. Meshing size of elements in in bonding area is defined as 0.5 mm equally. For those parts of laminate beside the welding region, 35 elements with a growing ratio of 1.5 along the longitudinal direction (Y axis) are allocated.

The predominate mechanism of heat transfer in the welding stack is expressed by the equation:

$$\rho C_p \left(\frac{\partial T}{\partial t} + u \nabla T \right) + \nabla \cdot q = Q \quad (1)$$

$$q = -k \cdot \nabla T \quad (2)$$

Where, ρ is the density (kg/m^3), C_p is the specific heat capacity at constant stress ($\text{J}/(\text{kg} \cdot \text{K})$), $u = 0$ is the velocity vector (m/s) as in this study welding process is in static condition, q is the heat flux by conduction (W/m^2), k is thermal conductivity ($\text{W}/\text{m} \cdot \text{K}$), and T is temperature (K). The thermal conductivity used in this model is temperature-dependent to precisely characterise heat transfer features.

Figure. 1(c) depicts the location of thermocouple for temperature validation to heat transfer model. Although thermocouple is more ideal to be placed at welding zone to monitor melting conditions, the existence of thermocouple wires (~ 1.2 mm) may disturb temperature distribution slightly. In addition, electric currents may flow into thermocouples when they come into touch with heating element, which may lead to reading errors of temperature.

An important indication of successful welding is to achieve as high as possible temperature for melting materials while avoiding materials degradation due to overheating. According to previous

3.2 Thermal evolution on welding interface

To clearly demonstrate the melting degree of materials on welding interface, the temperature map has been transformed into a phase change or melting degree map as depicted in Figure 3, where values from 0 to 1 represents non-melt to full-melt conditions. The melting degree of material at the interface between adherends and interlayer material was analysed. Generally, the melting at the interface will determine whether composite parts are successfully joined or not. Temperature map in XoY symmetric plane of heating element was also observed, where the highest temperature could be found. By monitoring temperature on that plane, welding parameters are fixed when highest temperature approached degradation point, and the maximum melting degree was also recorded.

The sets of graphs in Figure 3 (a) to (e) illustrate the melting evolutions in lap shear joint using defined welding parameters. To characterise the melting conditions, parameters established for this study were 200.3 kW/m^2 and 288.5 kW/m^2 for power density (PD) and 1.2 mm, 1.5 mm, 2 mm, and 4.5 mm for clamping distance (CD). The simulation results revealed two main types of melting evolution from Figure 3 (a) to (e). In Type 1 the melting of material initiated from the left and right side, extended into central area and then filled up the top and bottom sides slowly as shown in Figure 3 (a). The type 2 contrasting to type 1, started melting from the central area as shown in Figure 3 (b). Similarly, those top and bottom ends were the latest to melt.

From Figure 3 (a), the melting of material started from two sides after 18 seconds heating but was magnificently growing up in the next 4 seconds. This fast growth in temperature was then kept until the 30th second and slowed down after that. During the period from 30 s to 42 s, melting area along the bonding line continued with the slow rate by which the increment was less than 5 % (imaging area measured using software 'ImageJ'). Finally, after 61s, the welding interface has been completely melted. It was estimated that over 90% of melting were completed in the first 30 seconds, but it took another 31 seconds for fulfilling the full melting, especially melting the lower end. The reason is that the rest part of the adhered adjacent to bonding area continuously absorb heat from the lower end of bonding line due to the existence of high thermal gradient around this area. Moreover, while melting degree increased very slow during the last 31 seconds, temperature inside heating elements climbed swiftly. As shown in Figure 3(a), the temperature map shows that maximum temperature increased from 447.6°C to 502.8°C in that period, which led to a thermal degradation of polymers. In other words, the 100 % melting degree was just achieved. The low melting degree on top and lower ends could be a cause of low lap shear strength as high stress concentration was regarded emerging in those areas [21].

Thermal evolution of welding with CD of 1.5 mm and PD of 200.3 kW/m^2 is shown in Figure 3 (b). A shortened CD compared to results in Figure 3 (a), causing melting initiating from the centre, growing along both the horizontal and the vertical directions, and then expanding towards the four corners. Likewise, the maximum melting degree was obtained when processing after 30 seconds and after which degradation of material was detected. However, besides different transferring type, the melting degree of welds at 22nd second is $\sim 10\%$ lower than the case in Figure 3(a). That might cause a higher temperature difference within the welds. In addition, this set of PD and CD needs more time to reach the full melting by 67 seconds, though it is not necessarily a criterion to judge mechanical performance as material has already been degraded.

In Figure 3 (c), welding was operated with PD of 288.5 kW/m^2 and CD of 1.5 mm. The thermal propagation was similar to that shown in Figure 3 (a). However, in this 'quasi-Type 1' scenario, melting degree increased more evenly referring to the 2nd stage melting evolution. As another comparison to this potential optimum scene, welding was simulated with 288.5 kW/m^2 PD and 1.2 mm CD and results were depicted in Figure 3 (d). Welding by this scheme presented a type 2 welding again. However, after 16 second heating, melting degree of material was more evenly distributed by case (c) rather than case (d), and less time (2 seconds) was required to complete full melting for case (c).

Furthermore, welding using very long clamping distance was investigated and concluded as not acceptable. For example, heating with PD of 288.5 kW/m^2 and CD of 4.5 mm, as shown in Figure 3 (e), at 4th second temperature was up to 463°C inside the bonding region while the melting percentage was at extremely low level.

In general, high-quality welding essentially desires a high percentage of melting on the welding surface while avoiding material degradation. The simulation results indicate that those two parameters

need to be combined for analysis when considering their effects. Mismatching one of them, especially the one in Figure 3 (e) might lead to pre-mature thermal degradation.

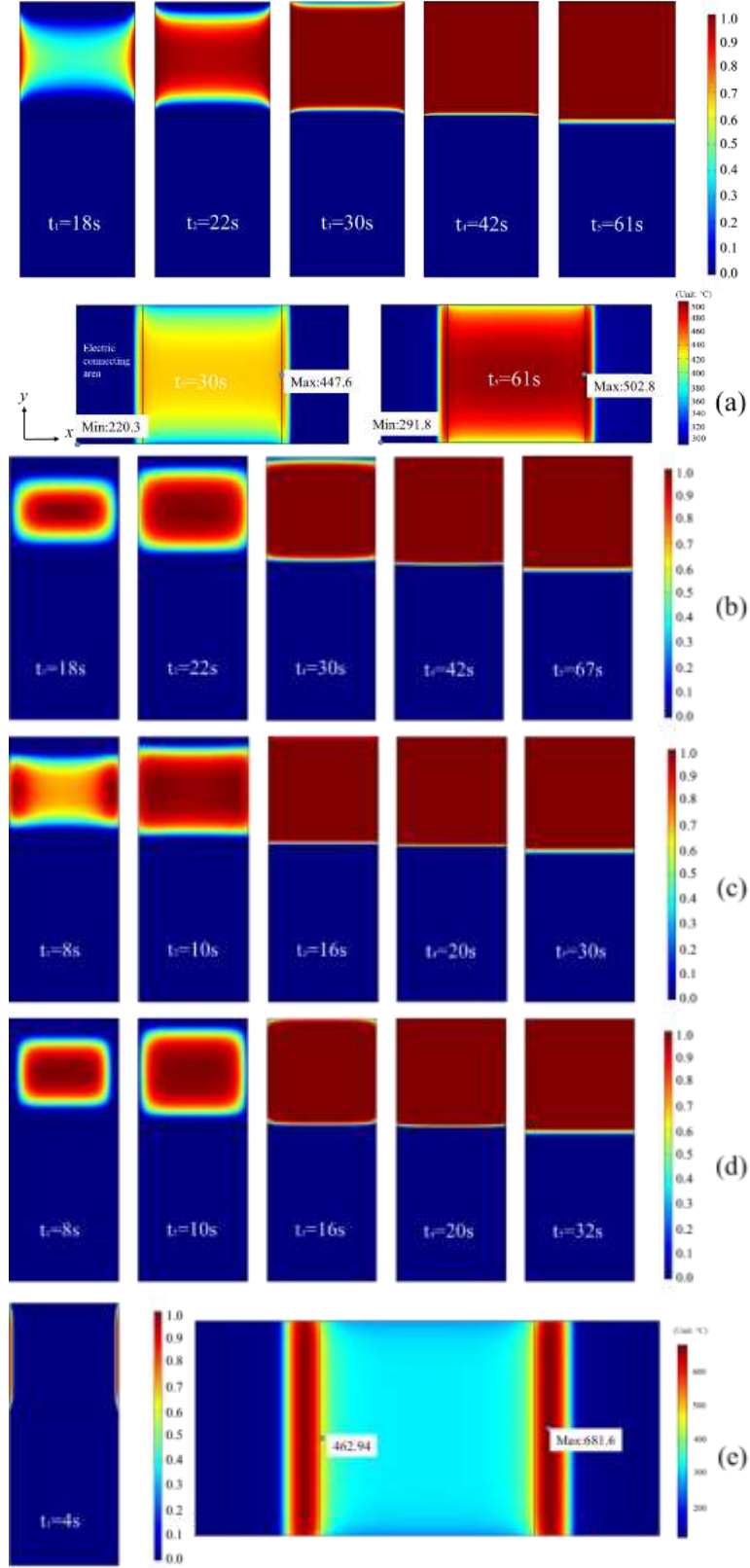


Figure 3: The melting process and evolution of phase changes in joining area, varying with time (a) CD = 2 mm, PD = 200.3 kW/m² (b) CD = 1.5mm, PD = 200.3 kW/m²; (c) CD = 1.5mm, PD = 288.5 kW/m² (d) CD = 1.2mm, PD = 288.5 kW/m² (e) CD = 4.5mm, PD = 288.5 kW/m²

3.3 Thermal evolution through laminate

Following results on welding interface, heat transferring through the thickness (along 'Z' axis) of the composite adherends was also observed. At different time steps corresponding to Figure 3 (a), melting condition on the sectional surface was depicted in Figure 4. During the period of reaching melting degree from 90% to 100%, the increment of melting penetration through the thickness had been nearly tripled (see Figure 4, t_3 and t_5). The main reason is that due to the inherent mechanism of heat conduction, heat was easier to be transferred to where there was large gap of temperature gradient according to Equation 1 and Equation 2.

The high rate of melting through thickness might incur the decrease of viscosity and modulus of matrix material, which then can be a cause of structure instability of laminate when pressures applied on welding area. Consequently, this flowing polymer will then result in fibre swapping and molten polymer being squeezed out. It was therefore necessary to consider the volumetric heat propagation as a key factor.

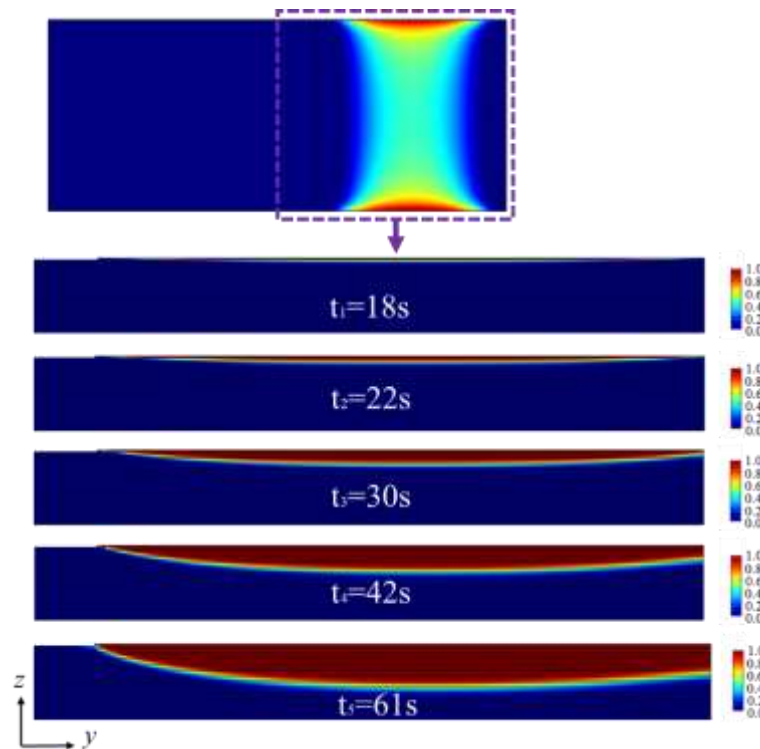


Figure 4: Thermal penetrating through laminates with processing parameters of CD = 2 mm and PD = 200.3 kW/m².

3.4 Assessment of parameters and testing results

Following the above-mentioned heat transfer analysis, simulations of the maximum melting percentage at the interface and thermal penetration through laminate are conducted with various combinations of power density and clamping distance. The results from 21 sets of welding simulations are listed in Table 1.

From Table 1, welding with the CD in the range of 1 mm to 1.5 mm benefit good melting degrees, with which bonding area melts between 93.1% and 97.2%. When clamping distance rises to 2 mm, the melting performance is maintained at an acceptable level with PD of 200.3 kW/m². However, the maximum melting degree reduces by more than 18.7 % within rising power levels up to 288.5 kW/m². For welding with short CDs, the average melting percentage is lower than 90%, which is not an ideal target.

It can be concluded that a good combination of power density and clamping distance will improve the melting process and avoid material degradation. Among those 21 sets, the welding with CD of 1.5

mm and PD = 392.7 kW/m² seems to be the most optimum. The maximum melting area is up to 97% within 7 seconds and the smallest penetration depth is 0.31 mm. However, in practice such high-power density can also be a risk because the tolerance for error is extremely limited. In general, a reliable welding is recommended to be done by choosing the power density from 251.3 kW/m² to 288.5 kW/m² and the clamping distance from 1.2 mm to 1.5 mm.

Regarding the heat penetrating depth, power density is the dominant factor. Typically, higher power density will induce less heat penetration through the composite laminate.

Therefore, experimental works were carried out using the optimum parameters obtained from the analysis of the simulation results. The results showed that the highest lap shear strength is 41.3 ± 4.9 MPa by Group 14, and within the range of recommended parameters, the other two welds (Group 16 and 12) achieved lap shear strength of 40.1 ± 3.7 MPa and 38.7 ± 4.1 MPa, respectively. Though the improvement of group 12 is not evidently advantageous, higher melting degree still dominates joint strength from the results. On the other side, material degradation is completely unacceptable, which leads to a lower strength of 26.7 ± 5.3 MPa. It is worth noting that the penetration depth seems not to be the predominant factor impacting lap shear strength. This might be because the application of glass board in welding effectively prevent structure movements in high melting degree condition. Finally, due to the limited size of lap shear specimen, the effect of this penetration and high thermal gradient within welds is not easy to detect.

Table 1: Design of parameters in the application to welding processes and performance assessment.

Group No.	Power density (kW/m ²)	Clamping distance (mm)	Time processed (s)	Maximum melting percentage	Penetrating depth (mm)	SL Strength (MPa)
1	200.3	0.5	36	89.8%	0.95	N/A
2	251.3	0.5	20	88.0%	0.73	N/A
3	288.5	0.5	15	87.6%	0.61	N/A
4	392.7	0.5	7	86.8%	0.41	N/A
5	200.3	1	36	94.5%	0.94	N/A
6	251.3	1	20	93.5%	0.63	N/A
7	288.5	1	15	93.4%	0.54	N/A
8	392.7	1	7	93.1%	0.31	N/A
9	200.3	1.2	36	96.3%	0.98	N/A
10	251.3	1.2	20	95.7%	0.64	N/A
11	288.5	1.2	25	Degraded	N/A	26.7 ± 5.3
12	288.5	1.2	16	95.4%	0.54	38.7 ± 4.1
13	392.7	1.2	7	96.5%	0.30	N/A
14	200.3	1.5	37	96.9%	0.96	41.3 ± 4.9
15	251.3	1.5	20	96.4%	0.65	N/A
16	288.5	1.5	15	97.2%	0.53	40.1 ± 3.7
17	392.7	1.5	7	97.0%	0.31	N/A
18	200.3	2	32	95.0%	0.78	N/A

19	251.3	2	16	90.1%	0.67	N/A
20	288.5	2	10	76.3%	0.28	N/A
21	392.7	2	4	25.2%	0.19	N/A

4 CONCLUSIONS

The resistance welding of thermoplastic composites has been studied with computational and experimental methods. The effect of different combinations of power densities and clamping distances on the temperature distribution along both the in-plane direction and the thickness direction of the welding area was investigated. The simulation results are successfully validated by the practical experiment, through the measurement of temperature evolution with a thermal meter and single lap shear tests. The optimum welding conditions in PD and CD were confirmed to be within the ranges from 251.3 kW/m² to 288.5 kW/m² and from 1.2 mm to 1.5 mm, respectively. Due to the limited size of the lap shear samples, the effect of the heat penetration along the thickness direction on the welding quality was not experimentally detected. The findings and investigating approaches in this study can provide informative knowledge to the researchers working in the field of resistance welding thermoplastics-based composites.

5 FUTURE WORK

Continuous optimisation of parameters for this heating resistors will be encouraged by using more efficient learning instead of changing factors individually to achieve better performance. Impacts for residual stress induced from thermal gradient is expected to investigate based on large scale samples.

REFERENCES

- [1] Koumoulos EP, Trompeta A-F, Santos R-M, Martins M, Santos CM dos, Iglesias V, et al. Research and Development in Carbon Fibers and Advanced High-Performance Composites Supply Chain in Europe: A Roadmap for Challenges and the Industrial Uptake. *J Compos Sci* 2019;3:86. <https://doi.org/10.3390/jcs3030086>.
- [2] Liu Y, Du S, Micallef C, Jia Y, Shi Y, Hughes DJ. Optimisation and Management of Energy Generated by a Multifunctional MFC-Integrated Composite Chassis for Rail Vehicles. *Energies* 2020;13:2720. <https://doi.org/10.3390/en13112720>.
- [3] Shi Y, Wang X, Wang F, Gu T, Xie P, Jia Y. Effects of inkjet printed toughener on delamination suppression in drilling of carbon fibre reinforced plastics (CFRPs). *Compos Struct* 2020;245:112339. <https://doi.org/10.1016/j.compstruct.2020.112339>.
- [4] Shi H, Villegas IF, Octeau MA, Bersee HEN, Yousefpour A. Continuous resistance welding of thermoplastic composites: Modelling of heat generation and heat transfer. *Compos Part A Appl Sci Manuf* 2015;70:16–26. <https://doi.org/10.1016/j.compositesa.2014.12.007>.
- [5] Rohart V, Laberge Lebel L, Dubé M. Improved adhesion between stainless steel heating element and PPS polymer in resistance welding of thermoplastic composites. *Compos Part B Eng* 2020;188. <https://doi.org/10.1016/j.compositesb.2020.107876>.
- [6] Stavrov D, Bersee HEN. Resistance welding of thermoplastic composites-an overview. *Compos Part A Appl Sci Manuf* 2005;36:39–54. [https://doi.org/10.1016/S1359-835X\(04\)00182-4](https://doi.org/10.1016/S1359-835X(04)00182-4).
- [7] Ageorges C, Ye L, Hou M. Experimental investigation of the resistance welding of thermoplastic-matrix composites. Part II: Optimum processing window and mechanical performance. *Compos Sci Technol* 2000;60:1191–202. [https://doi.org/10.1016/S0266-3538\(00\)00025-7](https://doi.org/10.1016/S0266-3538(00)00025-7).
- [8] Eveno EC, Gillespie JW. Resistance Welding of Graphite Polyetheretherketone Composites: An Experimental Investigation. *J Thermoplast Compos Mater* 1988;1:322–38.

- <https://doi.org/10.1177/089270578800100402>.
- [9] McKnight SH, Holmes ST, Gillespie JW, Lambing CLT, Marinelli JM. Scaling issues in resistance-welded thermoplastic composite joints. *Adv Polym Technol* 1997;16:279–95. [https://doi.org/10.1002/\(SICI\)1098-2329\(199711\)16:4<279::AID-ADV3>3.0.CO;2-S](https://doi.org/10.1002/(SICI)1098-2329(199711)16:4<279::AID-ADV3>3.0.CO;2-S).
- [10] Hou M, Yang M, Beehag A, Mai YW, Ye L. Resistance welding of carbon fibre reinforced thermoplastic composite using alternative heating element. *Compos. Struct.*, vol. 47, Elsevier Science Ltd; 1999, p. 667–72. [https://doi.org/10.1016/S0263-8223\(00\)00047-7](https://doi.org/10.1016/S0263-8223(00)00047-7).
- [11] Brassard D, Dubé M, Tavares JR. Resistance welding of thermoplastic composites with a nanocomposite heating element. *Compos Part B Eng* 2019;165:779–84. <https://doi.org/10.1016/j.compositesb.2019.02.038>.
- [12] Ageorges C, Ye L, Hou M. Experimental investigation of the resistance welding for thermoplastic-matrix composites. Part I: Heating element and heat transfer. *Compos Sci Technol* 2000;60:1027–39. [https://doi.org/10.1016/S0266-3538\(00\)00005-1](https://doi.org/10.1016/S0266-3538(00)00005-1).
- [13] Patel P, Hull TR, McCabe RW, Flath D, Grasmeyer J, Percy M. Mechanism of thermal decomposition of poly(ether ether ketone) (PEEK) from a review of decomposition studies. *Polym Degrad Stab* 2010;95:709–18. <https://doi.org/10.1016/j.polymdegradstab.2010.01.024>.
- [14] Ageorges C, Ye L, Hou M. Experimental investigation of the resistance welding of thermoplastic-matrix composites. Part II: Optimum processing window and mechanical performance. *Compos Sci Technol* 2000;60:1191–202. [https://doi.org/10.1016/S0266-3538\(00\)00025-7](https://doi.org/10.1016/S0266-3538(00)00025-7).
- [15] Ageorges C, Ye L, Hou M. Experimental investigation of the resistance welding for thermoplastic-matrix composites. Part I: Heating element and heat transfer. *Compos Sci Technol* 2000;60:1027–39. [https://doi.org/10.1016/S0266-3538\(00\)00005-1](https://doi.org/10.1016/S0266-3538(00)00005-1).
- [16] Reis JF, Abrahao ABM, Costa ML, Botelho EC. Assessment of the interlaminar strength of resistance-welded PEI/carbon fibre composite. *Weld Int* 2018;32:149–60. <https://doi.org/10.1080/09507116.2017.1347329>.
- [17] Hou M, Ye L, Mai YW. An Experimental Study of Resistance Welding of Carbon Fibre Fabric Reinforced Polyetherimide (CF Fabric/PEI) Composite Material. *Appl Compos Mater* 1999. <https://doi.org/10.1023/A:1008879402267>.
- [18] Yamane T, Katayama S, Todoki M, Hatta I. The measurements of thermal conductivity of carbon fibers. *J Wide Bandgap Mater* 2000;7:294–305. <https://doi.org/10.1106/QLXQ-CADP-HC2M-F14U>.
- [19] Talbot É, Hubert P, Dubé M, Yousefpour A. Optimization of thermoplastic composites resistance welding parameters based on transient heat transfer finite element modeling. *J Thermoplast Compos Mater* 2013;26:699–717. <https://doi.org/10.1177/0892705711428657>.
- [20] Hou M, Yang M, Beehag A, Mai YW, Ye L. Resistance welding of carbon fibre reinforced thermoplastic composite using alternative heating element. *Compos Struct* 1999;47:667–72. [https://doi.org/10.1016/S0263-8223\(00\)00047-7](https://doi.org/10.1016/S0263-8223(00)00047-7).
- [21] Liu Y, Lemanski S, Zhang X. Parametric study of size, curvature and free edge effects on the predicted strength of bonded composite joints. *Compos Struct* 2018;202:364–73. <https://doi.org/10.1016/j.compstruct.2018.02.017>.